The United Nations University

GEOTHERMAL TRAINING PROGRAMME
Orkustofnun, Grensasvegur 9,
IS-108 Reykjavik, Iceland

Reports 1994
Number 2

THE GEOCHEMISTRY OF THE MAHANAGDONG SECTOR, TONGONAN GEOTHERMAL FIELD, PHILIPPINES

Cecilia Polo Balmes
Geothermal Division, Energy Resource Development Bureau,
Department of Energy,
PNPC Complex, Merritt Road, Fort Bonifacio,
Makati, Metro Manila,
PHILIPPINES

ABSTRACT

In this report water geochemistry is used to evaluate the properties of waters from five wells and nine springs in the Mahanagdong sector of the Tongonan geothermal field. The spring waters can be classified into two groups, the alkali chloride waters of Bao, Banati 1 and the wells, and the steam-heated waters of Paril and Hanipolong springs. Based on quartz and Na-K geothermometer temperatures, which are within ±25°C of measured downhole temperatures, the highest subsurface temperature of 290-325°C is predicted in well MG-3D. A slight cooling is experienced by fluids from well MG-5D, located to the southeast. The subsurface temperature estimate for this well is about 267°C. Mixing of the deep hot water with cold groundwater is suggested by the enthalpy-chloride mixing model, to give rise to the Bao and Banati 1 spring waters with 70 to 77% hot water component and subsurface temperature estimates in the range of 218-233°C. Boiling of fluids of the same origin as that of the well waters is also indicated. There is strong evidence that the upflow is near well MG-3D, which is located in the northeast part of the Mahanagdong sector. Further study, however, must be carried out to verify whether Bao and Banati 1 spring waters represent the outflow from the field.

1. INTRODUCTION

Severe power cuts on the island of Luzon in 1992 forced the Philippine government to speed up several geothermal energy utilization projects including the interconnection of Leyte, where there are substantial geothermal resources, to this island whose power demand is ever increasing. Submarine cables will be used to transmit the energy. The Greater Tongonan Geothermal Field (GTGF) will play a great part in this programme. In addition to the existing 112.5 MW_e Tongonan I, a total of 640 MW_e is needed for the Leyte-Cebu (200 MW_e) and Leyte-Luzon (440 MW_e) interconnections (Figure 1). The geothermal project, Leyte A, comprises those areas in the GTGF (Figure 2) that can provide power for the first 640 MW_e. Leyte B comprises any remaining areas.

The first 200 MW_e are projected to come from the Upper Mahiao and Malitbog areas (130 and 70 MW_e) and the next 440 MW_e will be from the Malitbog, Mahanagdong and Alto Peak areas (170, 165 and 80 MW_e, respectively). Using the usual separation and turbine inlet pressures, it is estimated that 520 MW of electricity could easily be supplied by the areas mentioned above, and the rest by other prospect areas in Leyte

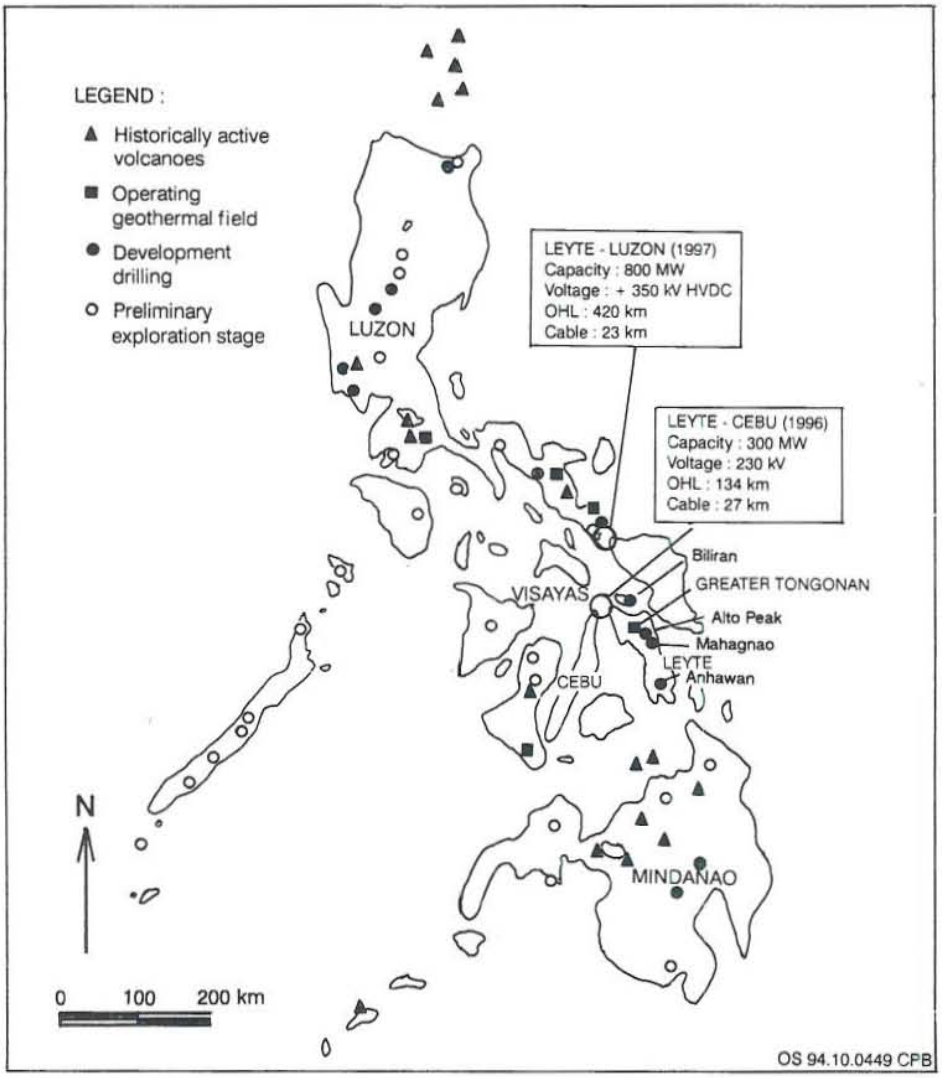

FIGURE 1: The Philippines, showing volcanoes, geothermal fields and planned interconnections using power from the Leyte A project

such as Biliran, Mahagnao and Anahawan. Optimization and maximization studies conducted by Sarmiento et al. (1992), Mesquite (1992) and Sarmiento et al. (1993) indicate that the Upper Mahiao and Malitbog sectors can be developed at pressures higher than those usually used for the geothermal turbines in the Philippines, i.e., 0.5 to 0.7 MPaa. The resource and process optimization and/or maximization of power generation indicates that the needed 640 MW can be available in the Greater Tongonan Geothermal Field if the turbine pressures were in the range of 1.0 to 1.2 MPaa. This strategy takes advantage of the benefits of increasing the thermodynamic and generation efficiencies that reduce specific steam consumption, i.e., kg/s of steam required per MW generated from high pressure turbines. This low specific steam consumption enables the optimization and maximization of the projected capacity estimates of Upper Mahiao, Malitbog and similarly Mahanagdong. Sarmiento et al. (1992) predict from the simulation that the field can sustain the higher pressures throughout its 25-year life, provided appropriate reservoir management strategies are adopted. These findings served as the basis of the PNOC-EDC plan to install the first high pressure geothermal turbines in the country (Sarmiento, 1993). The recommendation was based on the performance of the Tongonan I wells after 13 years of operation and the results of wellbore and reservoir simulation for the entire field.

This report focuses on the geochemical study of one of the above-mentioned areas, the Mahanagdong geothermal sector which has always been considered as a sink for the Mahiao-Sambaloran-Malitbog area. An initial hydrological model proposed by Lovelock et al. (1982) suggests the upflow to be in the Mahiao-Sambaloran sector with strong lateral flows to Malitbog and Bao-Valley (Sarmiento, 1993). However, recent studies indicate that the Mahanagdong-Paril area is a separate resource, as shown by tracer tests and other studies conducted in connection with the exploitation of Tongonan I.

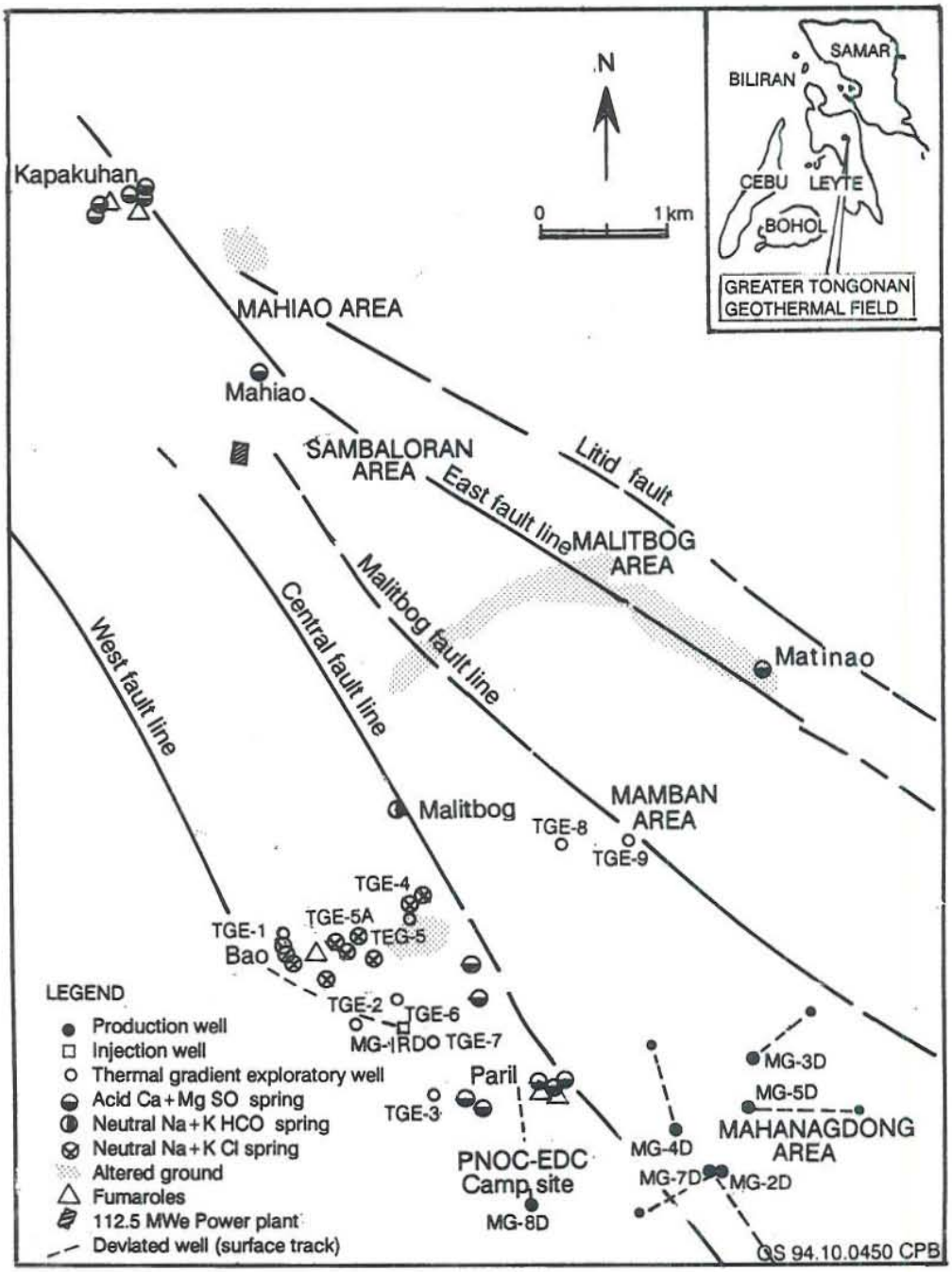

FIGURE 2: The Greater Tongonan Geothermal Field and the areas comprising it, the Mahiao-Sambaloran-Malitbog area and the Mahanagdong-Paril area; geothermal manifestations are shown for all areas, and boreholes in the Mahanagdong sector

It is the purpose of this report to construct a geochemical model of the area. Established geochemical tools, mostly for water chemistry, will be used to evaluate the fluids. As F. D'Amore stated, "Water geochemistry was already providing significant results more than 30 years ago, when it was pointed out that water-rock interaction and formation of hydrothermal alteration minerals from the rock matrix could, under determinate pressure and temperature conditions, be responsible for the composition of the liquid phase from what was originally a meteoric water. Laboratory experiments with water solutions have confirmed that an equilibrium exists between constituents in the liquid phase and alteration minerals. This equilibrium seems to be reached within a short geological time, even at relatively low reservoir temperatures" (D'Amore, 1991).

2. REVIEW OF PREVIOUS STUDIES

2.1 Geoscientific studies

The Mahanagdong sector is located 5 km southeast of the contiguous Mahiao-Sambaloran-Malitbog system. It is separated from the latter by the Mamban sector, a cooling reservoir block (PNOC-EDC, 1991). Major branches of the Philippine Fault Zone, trending NW-SE, run across the area.

A tentative analysis based on results for the few wells drilled in the sector show that hot aquifer fluids are channelled by the following fault lines: Paril, Northwest Paril, Central Fault Line, Mahanagdong, Malitbog and Malitbog Splay South (Figure 3). The Central Fault Splay and Mamban Fault copiously conduct cool and diluted fluids down to 2200 and 1200 m, respectively. Fault I, Central Fault Conjugate and M-B are associated with shallow intensely acid fluids, which appear to dissipate with depth. The results of fluid inclusion studies suggest that the Malitbog Splay South and M-D faults of MG-5D channel fluids that may contain high dissolved CO_2 concentrations. The Central Fault Splay and Mantugop may also harbour gassy fluids.

The relative permeabilities, deduced from the characteristics of the wells, are little known, except for that of the Central Fault Splay, which is moderately to highly permeable.

The surface rock outcrops in the Mahanagdong sector is composed of the Mahanagdong Volcanics, which are divided into older and younger volcanics. These are principally andesites thought to be comparable in age to the Sambaloran Volcanics. Mahanagdong Volcanics were predominant in the upper part of all the wells drilled in Mahanagdong.

The stratigraphic column for Mahanagdong is similar to that for Mahiao-Sambaloran and Malitbog except for some differences in lithology and contacts between formations. This consists of five formations, the Sambaloran and Mahanagdong Volcanics (SMV), North Central Leyte Formation (NCLF), Mamban Formation (MF), Bao Volcano-Sedimentary Formation (BVSF) and Mahiao-Sedimentary Complex (MSC). The stratigraphic column is characterized by products of andesitic volcanism, consisting of hornblende andesite, biotite-bearing hornblende andesite, and pyroxene hornblende andesite lavas and pyroclastics. Sedimentary formations consisting of sandstone, siltstone, claystone, shale, sedimentary breccia and dacite are encountered in the wells. The basement consists of several intrusions of a wide compositional range, from diorite to granodiorite (Bayrante et al, 1992; PNOC-EDC, 1991; Alvis-Isidro et al., 1993). Cross-sections through the Mahanagdong wells are shown in Figure 4 and a more detailed description of the formations in Table 1.

Microdiorite dykes in MG-1 appear to be related to the latest heat source at deeper levels but the series of dykes in MG-7D were apparently cold prior to the incursion of the latest hydrothermal fluids according to results of fluid inclusion studies (PNOC-EDC, 1991).

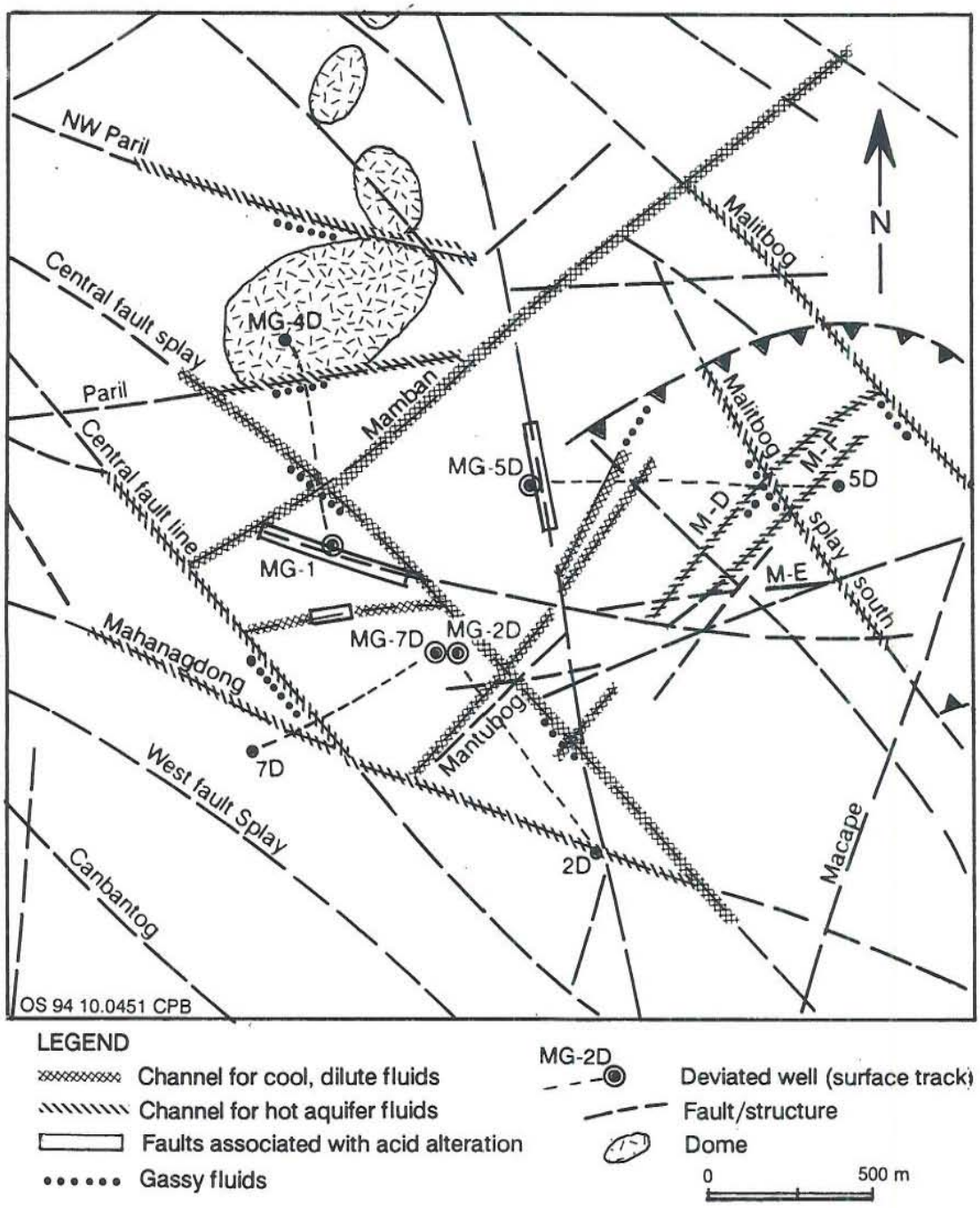

FIGURE 3: Mahanagdong, structures and their characteristics, also shown are the wells drilled in the sector (modified from PNOC-EDC, 1991)

Thermal manifestations in the area include the boiling, neutral Na+K chloride waters of the Bao and Banati springs. These are located at an elevation of 200-230 m a.s.l. in the northwest part of the field. Steam-heated waters can be found in the southeast and central parts such as the acid Ca+Mg sulphate hot springs, mud pools and steaming grounds at Mahanagdong at 490 m a.s.l., and the acid Ca+Mg sulphate bubbling pools at Paril at 370-400 m a.s.l. (PNOC-EDC, 1991). Major fault lines, thermal manifestations, and boreholes in the Mahanagdong sector are shown in Figure 2.

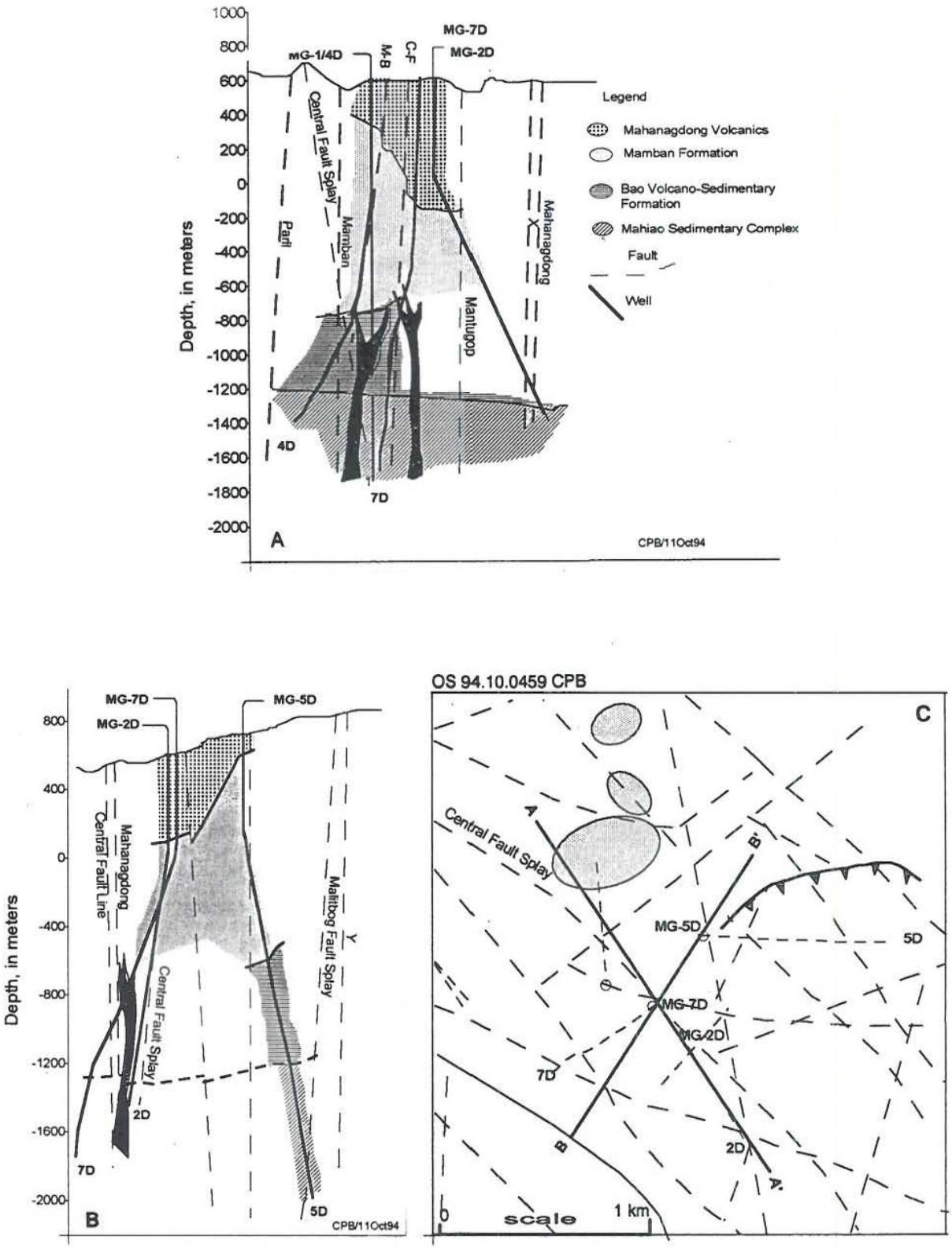

FIGURE 4: The stratigraphy of Mahanagdong wells; a) cross-section along line A-A'; b) cross-section along line B-B'; c) location of fault lines, wells and cross-sections

TABLE 1: The stratigraphic column of the Mahanagdong sector, Tongonan

FORMATION	AGE	DESCRIPTION	THICKNESS (m)	DIKE EVENTS	HYDROTHERMAL EVENTS
Mahanagdong Volcanics	Pleistocene to Recent	Series of andesite to silica andesite lava flows with varying percentages of augite, hornblende, hypersthene and biotite. Lavas are intercalated with minor tuff breccias. Basalt is rare.	150 - 760 m	3 Youngest	Latest Latest
NCLF* (MV)		Poorly sorted water laid tuff breccias intercalated with andesitic pyroclastics and lahars.	Confined to TGE wells; up to 580 m in TGE - 3		
Mamban Formation (MF)	Late Miocene to Pliocene	Majority consists of andesitic hyaloclastites with thin sedimentary layers of sedimentary breccia and (carbonaceous) sandy to silty claystone. Minor fossileferous limestones are allochtonous in MG-4D.	>985 m	4 Older	Earlier
Bao Volcano-Sedimentary Formation (BVSF)	Middle Miocene to Pliocene	Sedimentary breccias intercalated with lenses of completely recrystallized limestone and carbonaceous clayey siltstone to sandstone. Limestone was deposited in a shelfal environment but fossils are undiagnostic of age. Clasts are mostly andesites with minor basalt.	>550 m	Oldest	Earliest
Mahiao Sedimentary Complex (MSC)	Middle Miocene to Oligocene	Heterolithologic sedimentary breccias with a matrix of claystone and sandstone (now altered to illitic clays and chlorite). Clasts are dominated by microdiorite and diorite, with relatively minor andesite and basalt.	>520 m		

* North Central Leyte Formation

Schlumberger resistivity traversing (SRT) and vertical electrical sounding (VES) measurements conducted between 1974 and 1990 revealed two low resistivity zones with ≤ 10 to 30 ohmm bottom layers (Figure 5). The acid sulphate springs at Kapakuhan and the thermally altered ground at Mahiao, Sambaloran and some parts of Malitbog are within the first anomaly, while the chloride springs at Bao and Banati, the acid-sulphate waters at Hanipolong, Paril, Mahanagdong and the bicarbonate spring at Malitbog River near Barangay Tongonan are within the second. These two low resistivity zones are separated by an area of intermediate resistivities of 40 to 50 ohmm, which are attributed to the cold relict alteration within the Mamban Formation (Layugan et.al., 1990).

Geophysical and recent isotopic studies (Alvis-Isidro et al., 1993) revealed a distinct up-flow in Mahanagdong and despite a similar isotopic composition of the meteoric waters feeding the Tongonan geothermal system, the Mahanagdong reservoir is not hydrologically connected to the Mahiao-Sambaloran-Malitbog area. This is also confirmed by the fact that the Bao springs have not been significantly affected by the exploitation of Tongonan I. The results of tracer studies conducted at Sambaloran and Malitbog also indicated no connection between the two areas as tracers have neither been detected in the Bao springs nor in Tongonan geothermal exploratory wells.

2.2 Output measurements

To date, ten shallow exploratory wells in the Tongonan Geothermal Exploratory have been drilled and eight wells to over 1700 m vertical depth (VD). The eight wells are named: MG-1RD, MG-1, MG-2D, MG-3D, MG-4D, MG-5D, MG-7D and MG-8D. MG-1 was the first well drilled (spudded 11 July 1990) and MG-8D the latest (1993?). Well MG-1RD is intended as a reinjection well. All the wells have been discharged

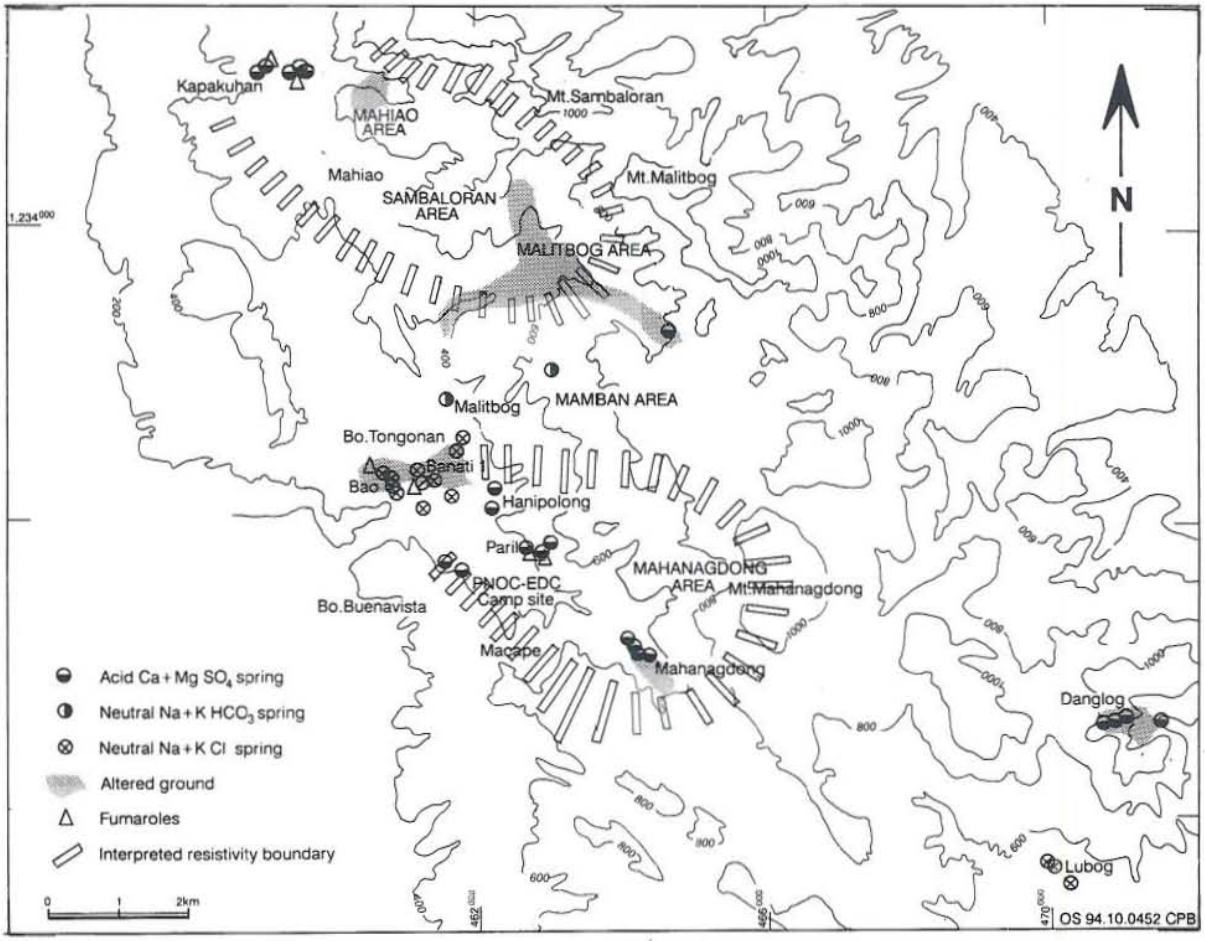

FIGURE 5: The two distinct low-resistivity zones detected in the Greater Tongonan Geothermal Field

except for wells MG-1RD and MG-8D. Well MG-4D discharged but the maximum wellhead pressure (WHP) attained was below the commercial value of 0.7 MPa. The measured injectivity was 77 l/s-MPa and the transmissivity 8 Dm. The mass flow was 20 kg/s and the enthalpy was less than 800 kJ/kg. Such a low enthalpy implies that the upper zone, with a feed temperature of about 140°C, is the one dominant during the discharge. After 21 days the discharge discontinued due to the formation of aragonite at the flash point (Urmeneta, 1993).

Well MG-8D is considered impermeable because of the high wellhead pressure encountered during fluid injection, the low injectivity index and the low transmissivity value, and likewise MG-1RD, in which no loss of circulation was observed during drilling.

All the wells except MG-1 need to be stimulated, either by two-phase stimulation or by air compression. Table 2 shows the results of completion tests for the wells that are included in this study. Injectivity tests showed that MG-7D has the highest injectivity at 157 l/s-MPa. During the transient pressure test, the pressure fall-off (PFO) response was minimal, suggesting very good permeability. Well MG-4D has a lower measured injectivity at 76 l/s MPa, but higher than wells MG-1, MG-2D, MG-3D and MG-5D (PNOC-EDC, 1991). As shown in the table, the wells have at least two permeable zones, with MG-3D having four. For wells MG-1 and MG-2D the main production zone is the upper one as indicated by the pivot point determined

TABLE 2: Completion test results for Mahanagdong wells

Parameter	MG1	MG2D	MG3D	MG5D	MG7D
Depth (m VD)	2335	2018	1860	2704	2293
WHP (Mpa-g)	1.1	1.1	0.9	0.8	1
Mass flow (kg/s)	90	94	72	30	100
Permeable zones (m VD)	1100-1300 1400-1600 2300-below	1180-1200 1500-1600 1800-2000	1300 1400 1929 near bottom	1200-1600 2200-2400	1335-1420 1460-1650
Inject. (l/s-MPa)	23	66	68	30	157
Transmiss. (Dm)	3.5	6	12	3.5	–
T max (°C)	270	272	>300	290	281

during heat-up and flowing surveys. While pivot points for wells MG-3D, MG-5D and MG-7D are not evident, it is believed that for well MG-3D it could be at 1629 m VD and for well MG-5D at 2200 m VD, as can be inferred from temperature surveys during flow. Well MG-7D may not be deep enough to reach the main productive zone. The liner could not be set at the bottom of the well due to an obstruction caused by a fish left in the hole.

Well MG-3D gave the highest measured temperature, about 300°C. It could be even higher, if it were not for the collapse of the formation during drilling, which forced the premature completion of the well. It has the highest power potential in the sector, 19 MW_e.

The most recent estimate of the extent of the system is 7.5 to 14 km^2, with the potential being moderately estimated to be 2675-4175 MW_eyears or 107-167 MW_e per year for a 25-year plant life. The sector is being developed to produce 165 MW_e.

3. METHODOLOGY

Using the WATCH programme, results of chemical analyses were evaluated. The WATCH (WATer CHemistry version 2.0, 1993) programme was used to evaluate the spring and well waters. This computer programme is an updated, unified version of WATCH1 and WATCH3 (Arnorsson et al.,1982) as revised by Bjarnason (1994). This new version uses the same thermodynamic data, but the FORTRAN code has been rewritten from scratch. It does the same calculations as the previous ones. It reads chemical analysis of water, gas and steam sample, and computes aqueous speciation, gas pressures, activity and solubility products, at the desired temperatures. The WATCH programme can also be used to compute the resulting species concentrations, activity coefficients, activity products and solubility products when the equilibrated fluid is allowed to cool conductively or boil adiabatically from the reference temperature to some lower temperature. This is particularly useful in the study of scaling. The computer programme WIN is used to create an input file for WATCH (Bjarnason, 1994).

Spring water samples included in this study were chosen for a good ionic balance, i.e., the percentage difference between the cation and anion concentrations determined, which should not be more than 5%, for the analytical chemical results. For this purpose WATCH was extensively used. Great care was taken to get representative samples from every important part of the Mahanagdong sector. Three springs from Banati

1, four from the Bao Valley, two from Hanipolong and two from Paril were selected. These springs were sampled in 1974 and 1983 and the results of chemical analysis are shown in Table 3. In addition to the spring water samples, five samples of well fluids are also included. The selection of a representative sample (Table 4) from each well was made on the basis of stable discharge chemistry and good ionic balance, with special emphasis on the latter as this represents the quality of the chemical analysis. It should always be remembered that the geochemical interpretation can only be as good as the sampling technique and the quality of the analysis.

TABLE 3: Chemical composition of selected spring waters in the Mahanagdong sector

Source	Date	ST °C	pH	CO2T	H2S	B	SiO2	Li mg	Na per	K kg	Mg	Ca	F	Cl	SO4	Ionic Bal. % diff.	Cl/B
BN1-177	11/14/83	96	8,05	0,00	0,70	23,80	242	4,78	1428	106	0,40	52,30	0,46	2367	73	-1,67	99
BN1-M193	05/19/74	97	7,94	9,38	0,00	36,70	276	7,60	2185	229	0,10	90,00	0,00	3606	78	1,46	98
BN1-M194	05/19/74	97	8,25	5,05	0,00	34,50	278	7,30	1990	211	0,40	86,00	0,00	3397	74	-1,84	98
BAO-179	11/14/83	98	7,31	0,00	0,50	36,00	289	6,83	2208	201	0,30	96,60	0,51	3863	107	-4,87	107
BAO-M196	05/19/74	99	8,05	9,38	0,00	36,60	258	7,20	2080	198	0,10	97,00	0,00	3560	83	-2,34	97
BAO-M198	05/19/74	100	7,85	14,43	0,00	35,50	250	6,90	2075	177	0,20	111	0,00	3511	84	-1,01	99
BAO-M200	05/19/74	99	8,24	10,82	0,00	34,40	245	6,80	2020	180	0,30	96	0,00	3383	81	-0,65	98
HP-194	11/16/83	66	6,53	nd	0,90	0,00	121	nd	19,00	6	6,80	35	0,14	2	219	–	–
HP-193	11/16/83	46	2,39	nd	0,60	0,00	215	nd	19,10	6	15,30	35	0,16	2	705	–	–
PR-204	11/16/83	56	3,97	nd	0,30	0,00	162	nd	35,20	8	11,80	75	0,10	4	490	–	–
PR-206	11/16/83	48	6,93	nd	0,00	0,10	58	nd	9,00	2	0,70	26	0,09	3	73	–	30

Notes:
ST - measured field temperature
BN1 - Banati 1
BAO - Bao
HP - Hanipolong
PR - Paril

TABLE 4: Representative discharge chemistry of Mahanagdong wells

Water phase

Source	Date	WHP bar abs.	SP	H (kJ/kg)	pH	CO2 T	H2S	NH3	B	SiO2	Li	Na	K	Mg	Ca	Fe	F	Cl	SO4	Ionic Bal. % diff.	Cl/B
									mg	per	kg										
MG1	05/0981	30,70	0,95	1211	8,06	2,76	0,05	0,00	59,00	851	8,50	2345	381	0,05	21,10	0,00	1,53	4065	37	-3,21	69
MG2D	10/30/81	11,34	0,95	1045	8,03	1,37	0,07	0,81	59,10	779	6,80	2281	412	0,09	26,40	0,13	2,05	3935	52	-1,68	67
MG3D	10/08/92	63,95	0,95	1894	7,32	8,44	0,40	3,42	45,80	1088	11,50	3519	938	0,13	110,30	0,23	1,75	6443	16	0,11	141
MG5D	08/26/83	16,40	0,95	1369	7.84	6,04	0,09	5,16	42,70	822	6,00	1993	296	0,07	17,70	0,16	0,54	3261	46	2,01	76
MG7D	01/15/91	28,00	0,95	1286	7,80	2,10	0,07	0,63	62,10	881	0,00	2400	457	0,04	25,30	0,10	0,00	4148	27	-0,65	67

Steam phase

	CO2	H2S	NH3	CO2 /H2S	CO2/NH3
	mg per kg				
MG1	15227	88,57	0,00	171,92	0,00
MG2D	7537	130,32	13,80	57,83	546,13
MG3D	46527	749,07	58,27	62,11	798,47
MG5D	33297	167,60	0.00	198.67	0,00
MG7D	11547	133,11	10,78	86.74	1071,11

Notes:
chemical composition of well fluids at atmospheric pressure
with CO2 and H2S calculated from steam phase and total flow
WHP = wellhead pressure
SP = sampling pressure
H = enthalpy

Besides WATCH, a computer programme called SPLITA (Bjarnason, pers. comm., 1994) was used. This programme computes the concentrations of CO_2 H_2S and NH_3 in any two of the following, steam, water, and total discharge, when the CO_2, H_2S, and NH_3 concentrations in the remaining phase are known, along with the steam fraction and the temperature. This is based on the vapour-liquid gas distribution coefficients and the specific volume of steam at a specified temperature. It was shown by Hulston and McCabe (1962) that the composition of gases released from New Zealand systems closely corresponds to that expected for gases completely dissolved in the deep liquid phase at a pressure corresponding to that of water vapour at the

equilibration temperature. Thus, by first calculating the concentration of the gases in the total flow, it was possible to express the chemical composition of well fluids at a common i.e., atmospheric pressure. In case of wells MG-3D, MG-5D and MG-7D, for example, even if CO_2, H_2S and NH_3 were analyzed in the water phase, these were disregarded and the steam phase concentrations of CO_2, H_2S and NH_3 collected at different pressures were calculated at atmospheric conditions, and the resulting concentrations of these gases in the different phases used for interpretation.

The waters were then evaluated using some well-known geochemical tools which were formulated on the classification of the components of the geothermal fluid into the reactive and non-reactive ones. Reactive components are those which participate in reactions between solution and hydrothermal minerals. Since the reactions are temperature and pressure dependent, the concentrations of such components provide information on the temperature of the geothermal system. Examples are Si, Na, K, Ca and Mg. Non-reactive or conservative components are those which do not participate in such reactions and thus, do not enter hydrothermal minerals. Once in the water constituents such as Cl, B, Li, Cs, and δD remain dissolved and can therefore be used as tracers for the origin or source of the fluid.

The Cl-Li-B triangular plot was specifically constructed to trace the origin and homogeneity of the fluid. Of the three components Li is least affected by secondary processes. Therefore, it can be used as a "tracer" for the initial deep rock dissolution process and as a reference to evaluate the possible origin of the other two important "conservative" constituents of thermal waters, Cl and B. Once added, Li remains largely in solution. At high temperatures Cl occurs largely as HCl, and B as H_3BO_3. Both are volatile and are mobilized by high temperature steam. They are, therefore, quite likely to have been introduced with the magmatic vapours that lead to the formation of the deep acid brine responsible for rock dissolution. At lower temperatures the acidity of HCl increases rapidly, and it is soon converted by the rock to the less volatile NaCl; B remains in its volatile form to be carried in the vapour phase even at relatively low temperatures.

The Cl-SO_4-HCO_3 diagram aids in the classification of waters. This diagram was constructed with reference to the sources of the three components Cl, SO_4, and HCO_3 and the processes undergone by the fluid containing them: the origin of Cl, for instance, can be traced from rainwater (and rock dissolution) and its "normal" occurrence in mature waters that arise from rainwater that has undergone water-rock interaction, and possibly evaporation and dilution with similar water; SO_4 and HCO_3 tend to derive from interfering processes such as, 1) the absorption of high-temperature CO_2 or H_2S - containing vapours into groundwater giving rise to "volcanic" or "steam-heated" waters, and 2) degassing and possibly biological processes resulting in "peripheral" waters.

The Cl-SO_4-HCO_3 diagram also allows the weeding out of unsuitable waters for the application of geoindicators. Caution is required for the application of most geoindicators to neutral, high bicarbonate waters, while for acid waters most geochemical techniques are not suitable. Chloride waters that plot along the Cl-HCO_3 axis, close to the Cl corner, are the group in which geochemical techniques can be applied with much confidence. Aside from determining the suitability of applying geochemical techniques, this diagram also provides an initial indication of mixing relationships or geographic groupings, with e.g. Cl waters forming a central core grading into HCO_3 waters towards the margins of a thermal area. High SO_4 steam-heated waters are usually encountered over the more elevated parts of a field. The degree of separation between data points for high chloride and bicarbonate waters gives an idea of the relative degrees of interaction of the CO_2 charged fluids at lower temperatures, and of the HCO_3 contents increasing with time and distance travelled underground.

The Na-K-Mg plot is employed to determine whether the fluid has equilibrated with hydrothermal minerals as well as to predict equilibration temperatures, $T_{Na\text{-}K}$ and $T_{K\text{-}Mg}$. Like the Cl-SO_4-HCO_3 diagram, the Na-K-Mg provides an indication as to the suitability of a given water for the application of ionic solute geoindicators. It is based on the temperature dependency of the full equilibrium assemblage of potassium

and sodium minerals that are expected to form after isochemical recrystallization of an average crustal rock under conditions of geothermal interest. The foregoing discussions on the three triangular plots used in this report were based on Giggenbach's (1991) treatment.

Geothermometer temperatures were calculated using the established silica and cation geothermometers listed in Appendix I. These geothermometers are based on the temperature and pressure dependency of hydrothermal reactions. All were used to calculate the reservoir temperature but some were instantly weeded out due to unrealistic results obtained i.e. K-Mg (Fournier, 1991) and Na-Ca and K-Ca (Tonani, 1980). The remaining or "reasonable" geothermometers, mostly Na-K developed by various authors were compared and evaluated together with those included in the WATCH programme.

Adiabatic boiling of the well waters at 25°C-intervals from the reservoir temperature to 100°C was simulated using WATCH. The resulting activity products (Q) for anhydrite, calcite, amorphous silica, chalcedony and quartz were divided by the equilibrium constant (K) at each temperature and the resulting logs of the (Q/K) ratios were then plotted against temperature. Reed and Spycher (1984) proposed this new approach to chemical geothermometry. D'Amore (1987) and D'Amore et al. (1987) have used this approach to obtain subsurface temperatures of spring waters in Sardinia and Venezuela, and obtained results that were in good agreement with conventional geothermometers. Tole et al. (1993) using data from 13 wells in Iceland showed that the approach can be used to indicate reservoir temperatures to within 20°C of measured aquifer temperatures. This approach is based on the theory that equilibrium constants vary strongly with temperature and are hardly affected at all by the pressures usually found in geothermal reservoirs, that is from 0-200 bars. The temperature at which a number of hydrothermal minerals converges is taken as the most likely aquifer temperature. Non-equilibrated waters will show no convergence of mineral solubilities to a common temperature while departure from equilibrium due to boiling or mixing with shallow colder waters is recognizable. Furthermore, this method validates the assumption of specific solution/mineral equilibria (Tole et al., 1993). This approach, however, could not be fully explored for the purposes of this report since aluminum concentrations are not available for any of the samples.

The enthalpy-chloride rather than the enthalpy-silica mixing model will be used to explain the processes taking place at depth in the fluids of the Mahanagdong sector. The enthalpy-chloride mixing model is more applicable where the mixed water emerges at boiling temperatures. The use of this model was originally described by Truesdell and Fournier (1976) using data from selected areas in Chile, New Zealand and Yellowstone Park. It was demonstrated that aquifer temperatures above the usual range of the silica geothermometer may be calculated from an enthalpy-chloride mixing model. Requirements for calculation include, 1) no loss or gain of steam occur before mixing takes place; 2) the temperatures resulting from mixing be within the range of accuracy of the quartz-saturation geothermometer (usually 150 to 205°C); 3) no precipitation of silica occur after mixing; and 4) no conductive loss of heat occur before or after mixing.

4. RESULTS AND DISCUSSION

4.1 Fluid chemistry

Results of chemical analyses of spring waters, presented in Table 3, show ionic balances that range from -4.86 to 1.46%. For well fluids ionic balances range from -3.21 to 0.11% (Table 4). There it is shown that the concentrations of the individual components fall within narrow groups. The mean chloride concentration of Banati 1 spring waters is 3123 ±663 ppm, and the Bao spring waters 3579 ±203 ppm. Excluding well MG-3D fluid, whose chloride concentration is 6443 ppm, that of all the other wells is 3852 ±404 ppm. Other major constituents like SiO_2, Na and K exhibit a similar pattern, their concentrations are highest in well MG-3D fluid followed by those of the other wells, then the Bao spring waters and the lowest in the Banati 1 spring

waters. The pH of Banati 1 well fluids and Bao spring waters ranges from 7.31 to 8.25. The pH of the Hanipolong and Paril spring waters on the other hand ranges from 2.39 to 6.93.

On the Cl-SO_4-HCO_3 triangular plot (Figure 6), Bao, Banati 1 and Mahanagdong well fluids plot on the chloride apex and Paril and Hanipolong fluids in the sulphate corner. Thus, it can be said that the well fluids from Banati 1 and Bao spring waters are neutral chloride waters, and Hanipolong and Paril spring waters are steam heated waters.

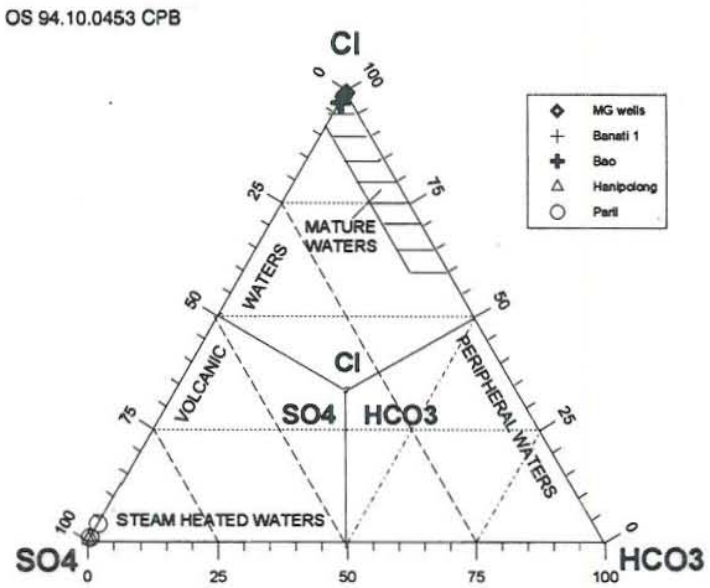

FIGURE 6: Cl-SO_4-HCO_3 diagram; alkali chloride spring waters and well fluids plot on the chloride apex and steam-heated waters in sulfate corner

Mass ratios like the Cl:B, Na:K, and Na:Li showed a narrow range for each group of spring waters suggesting a homogeneous fluid source at depth. A plot of relative chloride, lithium and boron concentration (Figure 7) shows that the fluids may originate from an old hydrothermal system. The boron content of thermal fluids reflects to some degree the maturity of a geothermal system. Like As, Sb and Hg, B is expelled during the early heating up stages because of its volatility. Therefore, fluids from "older" hydrothermal systems can be expected to be depleted in B. A slight deviation towards the upper left hand side of the Cl-Li-B plot can be seen, affecting MG-7D and MG-5D fluids. This is an indication that absorption of low B/Cl magmatic vapours may be taking place, probably from the same origin as that of the steam heated Paril spring.

It is shown in the Na-K-Mg plot of Giggenbach (1988) (Figure 8) that fluids from Bao springs have attained full equilibrium while the Banati 1 spring waters are in partial equilibrium. The well fluids, on the other hand, have attained full equilibrium. The position of the well fluids somewhat beyond the theoretical line is due to steam loss increasing absolute solute contents of samples collected at atmospheric pressure. On the original Na-K-Mg plot (Figure 9) the well fluids thus plot along a line marked "weirbox" (Giggenbach, 1991), i.e., waters boiled to 100°C.

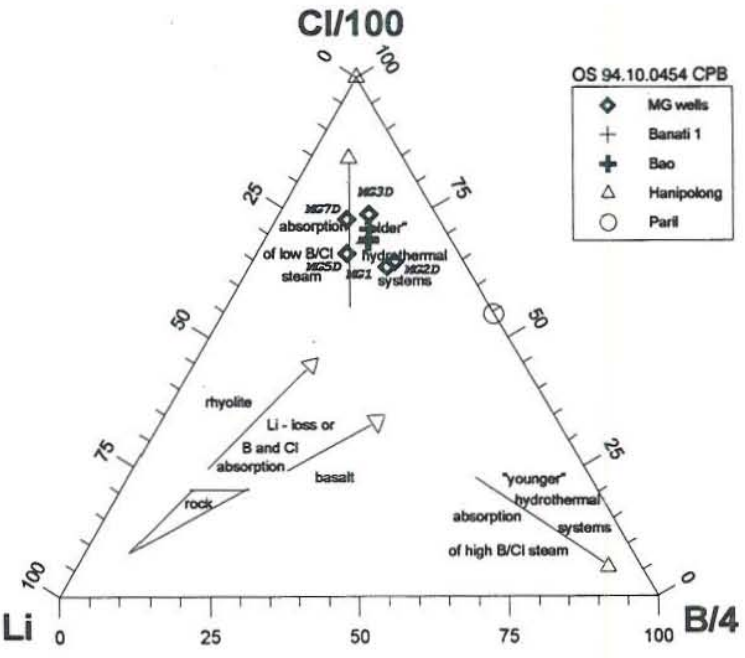

FIGURE 7: Cl-Li-B plot, showing that the Mahanagdong waters originate from an old hydrothermal system

4.2 Geothermometry

Table 5 shows results for the "reasonable" geothermometers used for the well and spring waters. These are the quartz, Na-K, and Na-K-Ca geothermometers. The choice of the

quartz geothermometer is based on the fact that in old rocks and in all rocks at temperatures >180°C quartz tends to be the controlling mineral, but in relatively young rocks at temperatures <180°C chalcedony may control the dissolution (Fournier, 1991). Since the Cl-Li-B triangular plot suggests that the waters have originated from an older hydrothermal system and all quartz temperatures are greater than 180°C, quartz can be assumed to be the controlling silica phase.

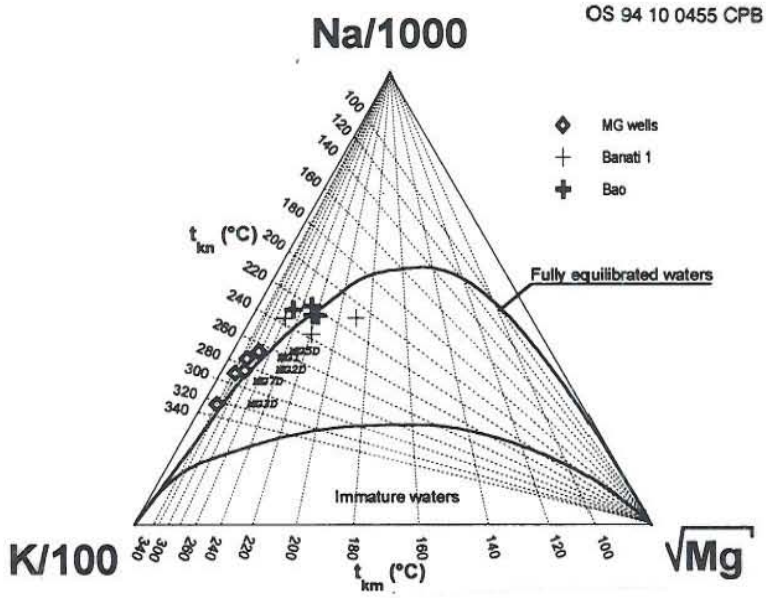

FIGURE 8: Plot of relative Na, K and Mg concentrations, showing that fluids from Bao springs and wells are in full equilibrium while those for Banati 1 are in partial equilibrium

The Na-K-Mg triangular plot indicates that the fluids have equilibrated with the sodium and potassium minerals. As such, the use of the Na-K geothermometers is justified. Subsurface temperature estimates range from 244 to 275°C for MG-1; 257 to 284°C for MG-2D; 290 to 342°C for MG-3D; 239 to 267°C for MG-5D; 264 to 289°C for MG-7D; 180 to 237°C for Banati 1 springs and 153 to 228°C for the Bao spring waters. The T_{NaK} of Giggenbach (1988) gave consistently the highest temperature estimate but the T_{NaK} of Truesdell (1976) the lowest, except in the case of MG-3D in which the lowest is from the T_{NaK} of Nieva and Nieva (1987) and the highest is from that of Tonani (1980). T_{NaK} temperatures differ by 25 to 39°C. The T_{NaKCa} results as well as the T_{SiO2} temperatures are within the T_{NaK} range.

Solubility curves for some minerals such as quartz, chalcedony, amorphous silica and anhydrite are shown in Figure 10. Mineral equilibrium diagrams for iron-containing minerals such as pyrrhotite, pyrite, goethite and magnetite were also drawn for the well fluids (Figure 11) except for well MG-1 fluid in which Fe was not detected. The absence of aluminum in the results of analysis limits the value of these curves for geothermometry. Nevertheless, some trends are apparent. The quartz and calcite curves, for instance, agree pretty well. In most cases they intersect the zero line at more than 260°C except for well MG-5D fluid where calcite suggests a higher equilibrium temperature. The anhydrite curves show under-saturation from 100°C to the temperature of quartz equilibration. However, it can also be speculated

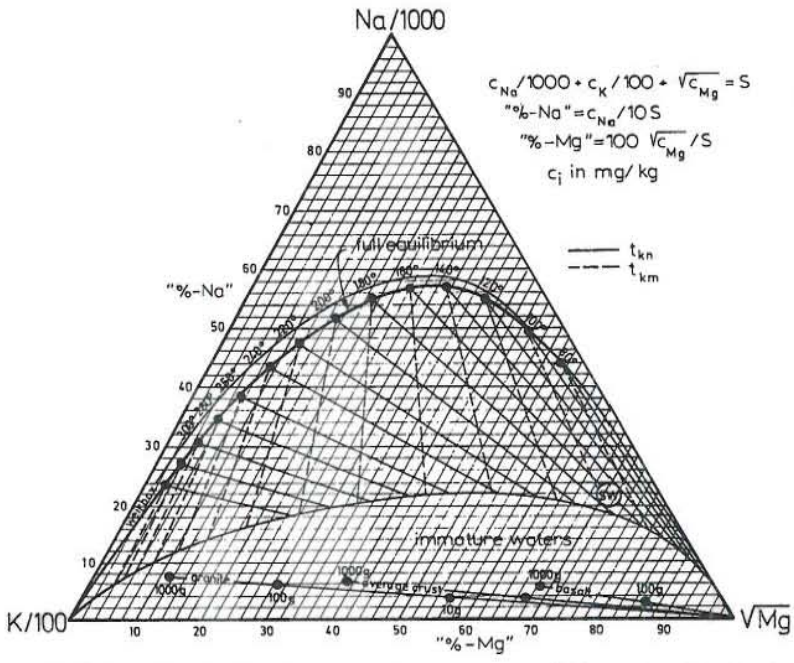

FIGURE 9: Na-K-Mg triangular diagram of Giggenbach (1991), well fluids would have plotted on the line marked "weirbox"

that they will intersect the zero line at about 325°C for wells MG-3D, MG-5D, and MG-7D; at about 290°C for well MG-2D fluid and at an even higher temperature for well MG-1. This behaviour of anhydrite suggests an older and/or deeper source temperature than quartz and calcite.

TABLE 5: Results of silica and NaK geothermometers in °C

Source	Quartz* F&P	NaK* SA	NaK AHT	NaK FT	NaK ROF	NaK N&N	NaK WFG	NaKCa F&T
Wells								
MG1	271	255	244	259	263	249	275	263
MG2D	264	265	257	274	274	259	284	268
MG3D	290	312	320	342	318	303	325	289
MG5D	267	244	231	245	253	239	266	254
MG7D	274	273	265	282	279	264	289	273
Springs								
BN1-177	192	169	155	163	193	180	210	195
BN1-M193	201	205	190	200	221	208	236	219
BN1-M194	199	206	191	202	222	209	237	218
Bao-179	207	189	175	184	209	196	225	209
Bao-M196	195	194	179	189	213	200	228	211
Bao-M198	193	183	168	177	204	191	220	203
Bao-M200	189	188	173	182	207	194	223	206

* - calculated by WATCH
F&P - Fournier and Potter, 1982
SA - Arnorsson et al., 1983
AHT - Truesdell, 1976
FT - Tonani, 1980
ROF - Fournier, 1979
N&N - Nieva & Nieva, 1987
F&T - Fournier & Truesdell, 1973
WFG - Giggenbach et al, 1983

Equilibrium diagrams for pyrrhotite, pyrite, goethite and magnetite (Figure 11) show that from an initial state of under-saturation at higher temperatures boiling brought about an increase in iron concentrations. The curves then intersect at temperatures ranging from about 180°C to 220±12°C. In almost all the well fluids except for that of well MG-3D, pyrite equilibrated in the highest temperature range; magnetite at about 200-212°C; pyrrhotite and goethite both equilibrated in the lowest temperature range. For well MG-3D fluid pyrrhotite equilibrated at the highest temperatures, about 235°C, and goethite at the lowest, about 185°C. It would be interesting to evaluate the behaviour of aluminum-containing minerals and see whether the equilibration temperatures will lean more towards the higher temperature estimate from anhydrite or towards that of quartz. However, on the basis of the various geothermometers previously discussed and the foregoing discussion on the available mineral equilibria diagrams, we can assume that temperatures greater than 325°C exist in the reservoir. It is also safe to assume that the highest subsurface temperature estimate is in the range of 290-325°C in MG-3D.

4.3 The enthalpy-chloride mixing model

The Cl:B ratio for all the spring waters is 98 ±0.75, except that for Bao-179 which is 107. For well fluids it is 69 ±4 except in MG-3D for which it is 141. The Na:K ratios are 11 ±2 for Banati 1 spring waters, 11 ±0.5 for Bao spring waters and 5.86 ±0.64 for waters from wells MG-1, MG-2D, MG-5D and MG-7D. That for MG-3D fluids is 3.75. These ratios suggest that mixing possibly took place during the ascent of the fluid to the surface.

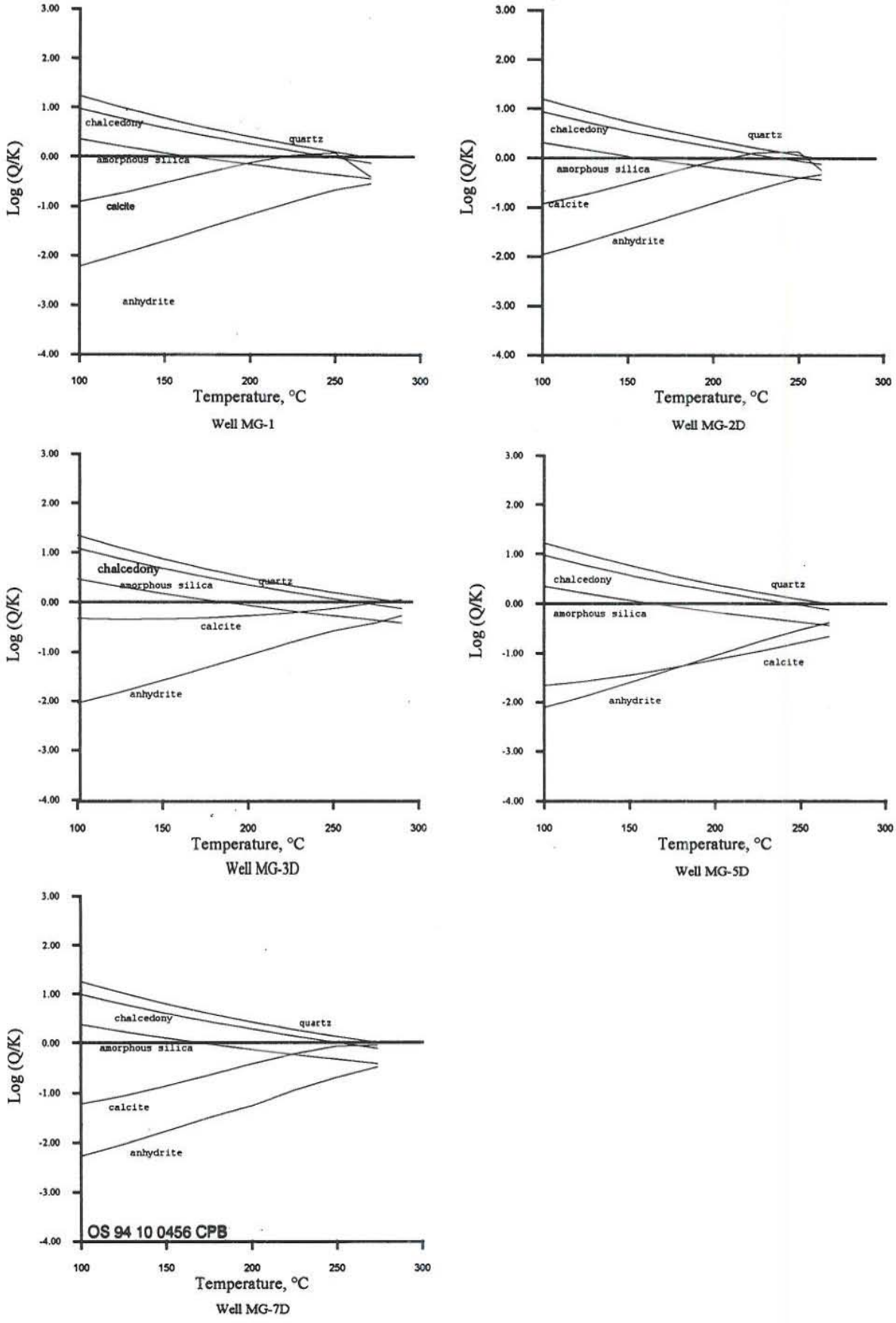

FIGURE 10: Mineral equilibrium diagrams for some minerals in the Mahanagdong well fluids

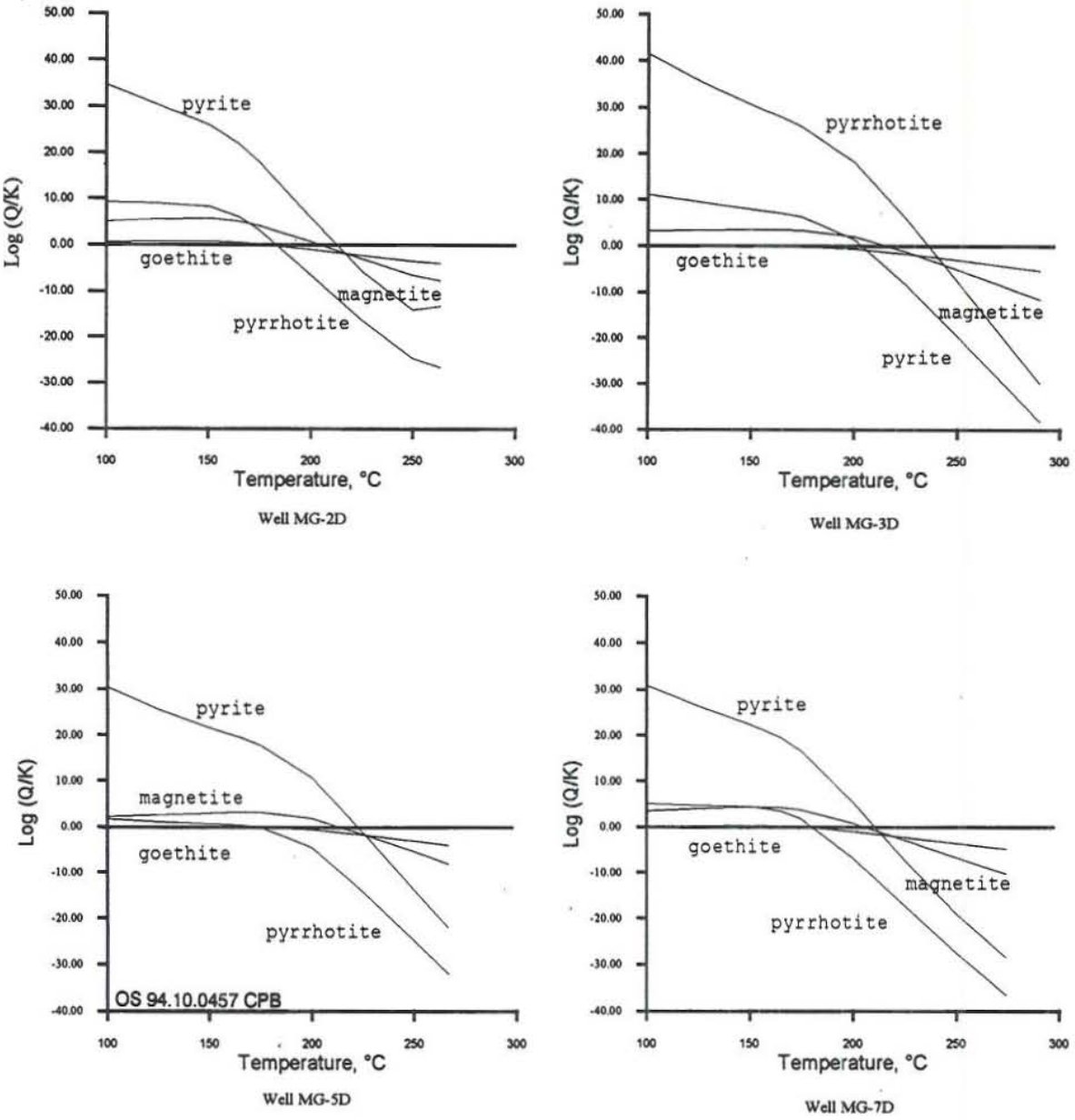

FIGURE 11: Mineral equilibrium diagrams for iron-containing minerals in the Mahanagdong well fluids

The enthalpy-chloride plot in Figure 12 shows that Bao and Banati 1 spring waters are mixtures of cold waters, and probably steam-heated waters, shown in the figure as line 1 (L1). The dilution line (L2) shows the possible enthalpy and chloride content of the springs that would result if the deep fluid from well MG-3D with an enthalpy of 1290 kJ/kg or a reservoir temperature of 290°C mixed with cold waters.

Lines were drawn from the springs to the steam composition of the inferred source of deep fluid. These lines represent the probable composition of the springs if they were to ascend adiabatically. When the enthalpy values corresponding to silica (quartz) geothermometry were plotted along the diagonal lines, almost all the points appear near the lower part of L2, except the one for spring BN1-177. A possible reason for these relatively low silica values is that silica might have polymerized and/or precipitated from the waters during their passage to the surface and before the sample collection took place. The high silica value and therefore the enthalpy of BN1-177 waters, on the other hand, might be due to non-equilibration of dissolved silica after

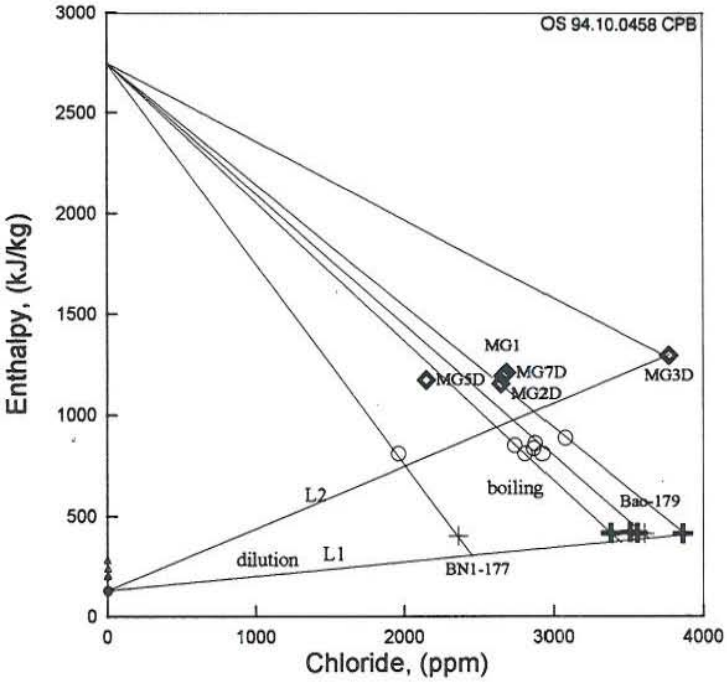

FIGURE 12: Enthalpy-chloride mixing plot for Mahanagdong waters

mixing (Truesdell and Fournier, 1976). After all, the boiling spring mixing model depends on assumed conservation of chloride and enthalpy and re-equilibration with quartz after mixing (Truesdell, 1976).

The chloride-enthalpy plot suggests that fluids from other wells are also more dilute than the fluid from MG-3D, with MG-2D and MG-5D experiencing a little cooling.

5. CONCLUSIONS

In this report water geochemistry was successful in delineating the most probable location of the up-flow of the deep hot water in the Mahanagdong sector. Well MG-3D fluid, with an estimated subsurface temperature that ranges from 290 to 325°C, represents the deep fluid, while wells MG-1, MG-2D, MG-5D and MG-7D waters are more diluted than the MG-3D fluid. The enthalpy-chloride mixing model showed that cold groundwater mixes with the deep fluid and that boiling of fluids, possibly originating from the same source as the well fluids, takes place to give rise to the Bao and Banati 1 spring waters. The enthalpy-chloride diagram also aided in the calculation of subsurface temperatures of boiling spring waters with mixed components. Assuming that well MG-3D tapped the source of the deep, hot fluid, calculation yielded: Bao-179 spring water, 233°C, 77% hot water; BN1-177, 177°C, 47% hot water; while all the other springs of about 218 °C have an approximately 72% hot water component.

While water geochemistry presents strong evidence that the up-flow is in the northeast part of the sector near well MG-3D, it is not clear if the Bao and Banati 1 springs on the northwest flank of the field, which are more diluted and colder, represent the outflow. Urmeneta (1993), cited that the outflow could not possibly be towards the Bao Valley, since wells MG-1RD and MG-8D that are drilled to the northwest are impermeable. This study, therefore, must be supplemented by other geochemical tools and/or other disciplines.

ACKNOWLEDGEMENTS

I would like to acknowledge the UNU and the Icelandic Government for the support extended to the UNU Geothermal Training Programme; Dr. Ingvar Birgir Fridleifsson and Mr. Ludvik S. Georgsson not only for providing me a slot in this fellowship but also for the assistance given all through the duration of the course (also to Ms. Margret Westlund); Dr. Jon Orn Bjarnason and my adviser, Dr. Halldor Armannsson, for the generous sharing of their time and knowledge; all the lecturers for their valuable teachings; the rest of the

Orkustofnun family for their hospitality especially Helga, Gudrun, Svanur and Lina; and to Julio who gave so much of his time in helping his classmates solve computer related problems.

Back home, I would also like to acknowledge Mr. Francisco A. Benito and Mr. Narciso V. Salvania for the support extended to me both at work and while on training and Hermes P. Ferrer and Rowena Alvis-Isidro of PNOC-EDC for providing me the data needed for this report.

REFERENCES

Alvis-Isidro, R.R., Solana, R.R., D'Amore, F., Nuti, S., and Gonfiantini, R., 1993: Hydrology of the greater Tongonan geothermal system, Philippines, as deduced from geochemical and isotopic data. *Geothermics (special issue on the Philippines), 22,* 435-449.

Arnorsson, S., 1983: Chemical equilibria in Icelandic geothermal systems. Implications for chemical geothermal investigations. *Geothermics, 12,* 119-128.

Arnorsson, S., Gunnlaugsson, E., and Svavarsson, H., 1983: The chemistry of geothermal waters in Iceland. III. Chemical geothermometry in geothermal investigations. *Geochim. Cosmochim. Acta, 47,* 567-577.

Arnorsson, S., Sigurdsson, S., and Svavarsson, H., 1982: The chemistry of geothermal waters in Iceland I. Calculations of aqueous speciation from 0°C to 370°C. *Geochim. et Cosmochim Acta, 46,* 1513-1532.

Bayrante, L.F., and Herras, E.B., 1990. *MG-4D geologic report.* PNOC-EDC, internal report.

Bayrante, L.F., Rodis, N.O., Reyes, A.G., and Sanchez, D.R., 1992: Resource assessment of the Mahanagdong geothermal project, Leyte, Central Philippines. *Proceedings of the 14th New Zealand Geothermal Workshop, University of Auckland,* 171-178.

Bjarnason, J.O., 1994: *The speciation programme WATCH, version 2.0.* Orkustofnun, Reykjavik.

D'Amore, F., 1987: Some geochemical techniques for reservoir temperature computations. *Proceedings of Intern. Symp. on Development and Exploration of Geothermal Resources,* Instituto Investigaciones Electricas, Comision de Comunicades Europeas, Cuernavaca, Mexico, 50-57.

D'Amore, F., 1991: Gas geochemistry as a link between geothermal exploration and exploitation. In: D'Amore, F. (co-ordinator), *Application of Geochemistry in Geothermal Reservoir Development* UNITAR/UNDP publication, Rome, Italy, 93-117.

D'Amore, F., Fancelli, R., and Caboi, R., 1987: Observation on the application of chemical geothermometers to some hydrothermal systems in Sardinia. *Geothermics, 16,* 271-282.

Fouillac, C., and Michard, G., 1981: Sodium/lithium ratios in water applied to geothermometry of geothermal reservoirs. *Geothermics, 10,* 55-70.

Fournier, R.O., 1979: A revised equation for the Na/K geothermometer. *Geoth. Res. Council, Transactions, 3,* 221-224.

Fournier, R.O., 1991: Water geothermometers applied to geothermal energy. In: D'Amore, F. (co-ordinator), *Application of Geochemistry in Geothermal Reservoir Development.* UNITAR/UNDP publication, Rome, Italy, 37-69.

Fournier, R.O., and Potter, R.W., 1982: A revised and expanded silica (quartz) geothermometer. *Geoth. Res. Council Bull., 11-10,* 3-12.

Fournier, R.O., and Rowe, J.J., 1977: The solubility of amorphous silica in water at high temperatures and high pressures. *Am. Min., 62,* 1052-1056.

Fournier, R.O., and Truesdell, A.H., 1973: An empirical Na-K-Ca geothermometer for natural waters. *Geochim. Cosmochim. Acta, 37,* 515-525.

Giggenbach, W.F., 1988: Geothermal solute equilibria. Derivation of Na-K-Mg-Ca geoindicators. *Geochim. Cosmochim. Acta, 52,* 2749-2765.

Giggenbach, W.F., 1991: Chemical techniques in geothermal exploration. In: D'Amore, F. (co-ordinator), *Application of Geochemistry in Geothermal Reservoir Development.* UNITAR/UNDP publication, Rome, Italy, 119-142.

Giggenbach, W.F., Gonfiantini, R., Jangi, B.L, and Truesdell, A.H., 1983: Isotopic and chemical composition of Parbati Valley geothermal discharges, NW-Himalaya, India. *Geothermics, 12,* 199-222.

Hulston, J.R., and McCabe, W.J., 1962: Mass Spectrometer measurements in the thermal areas of New Zealand. *Geochim. Cosmochim. Acta, 26,* 399-410.

Kharaka, Y.K., Lico, U.S., and Law, L.M., 1982: Chemical geothermometers applied to formation waters, Gulf of Mexico and California basins (abstract). *Am. Assoc. Petrol Geol. Bull., 66,* 588.

Kharaka, Y.K., and Mariner, R.H., 1989: Chemical geothermometers and their application to formation waters from sedimentary basins. In: Naeser, N.D., and McCollon, T.H. (eds.), *Thermal History of Sedimentary Basins.* Springer-Verlag, New York, 99-117.

Layugan, D.B., Catane, J.P.L., Maneja, F.C., Herras, E.B., and Vergara, M.C., 1990: *Resistivity surveys across the Tongonan geothermal field, Leyte.* PNOC-EDC, internal report, 33 pp.

Lovelock, B.G., Cope, D.M., and Baltazar, A.S.J., 1982: A hydrochemical model of the Tongonan geothermal field. *Proceedings of the Pacific Science Conference 1982, Auckland,* 259-264.

Mesquite, 1992: *Leyte 'A' geothermal project optimization. Review of improved resource performance and power generating strategies to the greater Tongonan geothermal field.* Report prepared for PNOC-EDC.

Nieva, D., and Nieva, R. 1987: Developments in geothermal energy in Mexico, part 12 - A cationic composition geothermometer for prospection of geothermal resources. *Heat Recovery systems and CHP, 7,* 243-258.

PNOC-EDC, 1991: *Resource assessment update: Mahanagdong sector, greater Tongonan geothermal field. Geoscientific Department.* PNOC-EDC, internal report, 73 pp.

Reed, M., and Spycher, N., 1984: Calculation of pH and mineral equilibria in hydrothermal waters with application to geothermometry and studies of boiling and dilution. *Geochim. Cosmochim. Acta, 48,* 1479-1492.

Sarmiento, Z.F., 1993: *Geothermal development in the Philippines.* UNU G.T.P., Iceland, Report 2, 99 pp.

Sarmiento, Z.F., Aquino, B.G., Aunzo, Z.P., Rodis, N.O., and Saw, V.S., 1992: *Optimizing the performance of the Tongonan geothermal reservoir.* PNOC-EDC, internal report.

Sarmiento, Z.F., Aquino, B.G., Aunzo, Z.P., Rodis, N.O., and Saw, V.S., 1993: An assessment of the Tongonan geothermal reservoir at high pressure operating conditions. *Geothermics (special issue on the Philippines), 22,* 451-466.

Tole, M.P., Armannsson, H., Pang Zhong-He, and Arnorsson, S., 1993: Fluid/Mineral equilibrium calculations for geothermal fluids and chemical geothermometry. *Geothermics, 22,* 17-37.

Tonani, F., 1980: Some remarks on the application of geochemical techniques in geothermal exploration. *Proceedings, Adv. Eur. Geoth. Res., 2nd Symp., Strasbourg,* 428-443.

Truesdell, A.H., 1976: Summary of section III, geochemical techniques in exploration. *Proceedings of 2nd United Nations Symposium on the Development and Use of Geothermal Resources, San Francisco, 1975, 1,* liii-lxxix.

Truesdell, A.H., and Fournier, R.O., 1976: Calculations of deep temperatures in geothermal systems from the chemistry of boiling spring waters of mixed origin. *Proceedings of 2nd United Nations Symposium on the Development and Use of Geothermal Resources, 1,* 837-844.

Urmeneta, N.N.A.,1993: *Natural state simulation of the Mahanagdong geothermal sector, Leyte, Philippines.* UNU G.T.P., Iceland, report 15, 31 pp.

APPENDIX I: Equations for silica and cation geothermometers

Geothermometer	Equation		Source
SiO_2 (Quartz)	$t\ °C = C_1 + C_2S + C_3S^2 + C_4S^3 + C_5 \log S$		Fournier and Potter (1982)
where	$C_1 = -4.2198 \times 10^1$	$C_3 = -3.6686 \times 10^{-4}$	$C_5 = 7.7034 \times 10^1$
	$C_2 = 2.8831 \times 10^{-1}$	$C_4 = 3.1665 \times 10^{-7}$	$S = SiO_2$, ppm
Na-K	$t\ °C = \frac{856}{0.857 + \log (Na/K)} - 273.15$		Truesdell (1976)
Na-K	$t\ °C = \frac{833}{0.780 + \log (Na/K)} - 273.15$		Tonani (1980)
Na-K	$t\ °C = \frac{933}{0.993 + \log (Na/K)} - 273.15$	(25-250°C)	Arnorsson (1983)
Na-K	$t\ °C = \frac{1319}{1.699 + \log (Na/K)} - 273.15$	(250-350°C)	Arnorsson (1983)
Na-K	$t\ °C = \frac{1217}{1.483 + \log (Na/K)} - 273.15$		Fournier (1979)

Na-K $$t\ °C = \frac{1178}{1.470 + \log (Na/K)} - 273.15$$ Nieva and Nieva (1987)

Na-K $$t\ °C = \frac{1390}{1.750 + \log (Na/K)} - 273.15$$ Giggenbach et al. (1983)

K-Mg $$t\ °C = \frac{2330}{7.35 - \log (K^2/Mg)} - 273.15$$ (for $\log (K^2/Mg) > 1.25$) Fournier (1991)

K-Mg $$t\ °C = \frac{1077}{4.033 + \log (K^2/Mg)} - 273.15$$ (for $\log K^2/Mg) < 1.25$) Fournier (1991)

K-Mg $$t\ °C = \frac{4410}{14.00 - \log (K/\sqrt{Mg})} - 273.15$$ Giggenbach (1988)

Li-Mg $$t\ °C = \frac{2200}{5.470 - \log (Li/\sqrt{Mg})} - 273.15$$ Kharaka & Mariner (1989)

Na-Li $$t\ °C = \frac{1590}{0.779 - \log (Na/Li)} - 273.15$$ Kharaka et al. (1982)

Na-Li $$t\ °C = \frac{1000}{0.389 - \log (Na/Li)} - 273.15$$ (Cl < 0.3 M) Fouillac & Michard (1981)

Na-Li $$t\ °C = \frac{1195}{0.130 - \log (Na/Li)} - 273.15$$ (Cl > 0.3 M) Fouillac & Michard (1981)

Na-Ca $$t\ °C = \frac{1096.7}{3.080 - \log (Na/Ca)} - 273.15$$ Tonani (1980)

K-Ca $$t\ °C = \frac{1930}{3.861 - \log (K/\sqrt{Ca})} - 273.15$$ Tonani (1980)

Na-K-Ca $$t\ °C = \frac{1647}{\log(Na/K) + \beta \log(\sqrt{Ca}/Na) + 2.06 + 2.47} - 273.15$$ Tonani (1980)

$B = 4/3$ for $t < 100°C$; $B = 1/3$ for $t > 100°C$